Hindawi
Modelling and Simulation in Engineering
Volume 2022, Article ID 6544820, 6 pages
https://doi.org/10.1155/2022/6544820

Research Article

Numerical Simulation of Single-Mode 3D Rayleigh-Taylor Instability

Dongyung Kim

Department of Mathematics, Phoenix College, Phoenix, AZ 85013, USA

Correspondence should be addressed to Dongyung Kim; dongyung.kim@phoenixcollege.edu

Received 21 September 2022; Revised 12 October 2022; Accepted 28 October 2022; Published 9 November 2022

Academic Editor: Houari Ameur

Rayleigh-Taylor instability (RTI) is analyzed theoretically by Taylor, and 2-dimensional experimental results are obtained by Lewis in 1950. Over the 72 years, several experiments and theories are developed with the shock-driven Ritchmyer-Meshkov instability (RMI) and the shear-driven Kelvin-Helmholtz instability (KHI). Here, we emphasize the single-mode Rayleigh-Taylor instability (RTI) mixing simulation with a surface area in 3 dimensions. The simulation uses concentration equations and nonzero transport. We observed chaotic interface behavior even for this single-mode simulation, in the sense that the interface appears to have an area proportional to Δx^{-1}, with respect to its mesh (non)convergence (i.e., rate of divergence) properties.

1. Introduction

Many important industrial problems involve flows with multiple constitutive components. Due to inherent nonlinearities and the complexity of dealing with unknown moving interfaces, multiphase flows are challenging. There are many ways to model moving interfaces. The two main approaches to simulating multiphase and multicomponent flows are interface tracking and interface capturing. In interface tracking methods (front-tracking [1], immersed interface [2], immersed boundary [3, 4]), Prometheus with PPM(the piecewise-parabolic method) [5], and CLAWPACK [6]), Lagrangian particles are used to track the interfaces. In interface capturing methods such as level-set [7, 8] and phase-field methods [9], the interface is implicitly captured by a contour of a particular scalar function. Another types of methods are Clawpack and Prometheus Method (PPM). Reference will be inserted. The numerical method we will take is Front-tracking method (FTM), which is originally developed by Glimm et al. [1] and Immersed boundary method (IBM), which is originally developed by Peskin [4]. The IBM was started to be applied to two-phase fluid flows [10–12], and the FTM was started to be applied to two-phase fluid flows. The motion of the fluid with the interface tracking method is influenced by the force generated by the interface, and the interface moves at the local fluid velocity. The strength of this method is accurate and robust with time-dependent geometry of the interface. See Figure 1 for 2-dimensional incompressible and immiscible two fluid mixing cases. Here, ρ is the variable density, and μ is the variable viscosity. $X(s, t)$ is the interface of two fluid mixing in 2 dimensions.

We extend the problems to a 3-dimensional space with compressible two fluid mixing cases. This problem is one of Rayleigh-Taylor instabilities (RTI) [13] with the density differences. RTI is applied to resolve supersonic ramjet [14] and scramjet or inertial confinement fusion (ICF) problems [15]. We consider the Navier-Stokes equations with transport for a mixture of two compressible species:

$$\frac{\partial \rho}{\partial t} + \nabla \cdot \rho \mathbf{v} = 0, \tag{1}$$

$$\frac{\partial \rho \mathbf{v}}{\partial t} + \nabla \cdot \left(\rho \mathbf{v}\mathbf{v} + p\delta_{ij}\right) = \nabla \cdot \mathbf{d}, \tag{2}$$

$$\frac{\partial E}{\partial t} + \nabla \cdot (E + p)\mathbf{v} = \nabla \cdot \kappa \nabla T + \nabla \cdot \mathbf{d} \cdot \mathbf{v}, \tag{3}$$

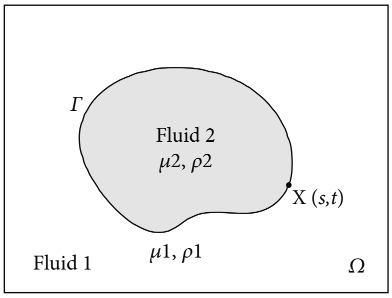

Figure 1: Front-tracking and Immersed boundary curve Γ on a rectangular domain Ω.

$$\frac{\partial \rho\psi}{\partial t} + \nabla \cdot \rho\psi\mathbf{v} = \nabla \cdot \rho\mu\nabla\psi. \quad (4)$$

The following are the dependent variables: ρ is the total mass density, $\mathbf{v}$ is the velocity, p is the pressure, E is the total energy, ψ is the species mass fraction, κ is the coefficient of heat conductivity, and μ is the molecular mass diffusion.

Equation (1) is the continuum equation, equation (2) is the momentum equation, equation (3) is the energy equation [16], and equation (4) is the mass fraction equation. In equation (4), we added and developed the volume fraction formulas to preserve the mass in the interface because it is not conservative in the interface, grid cell crossings and it is conservative without interface. After we add and develop the volume fraction formulas, it almost becomes conservative in the interface and grid cell crossing [17].

The equation of state (EOS) is defined for each of the species as a gamma law gas, and according to [18], the mixture EOS is a gamma law gas also. $\mathbf{d}$ is the viscous stress $\mathbf{d} = 2\nu[\mathbf{S} - (1/3)\mathrm{tr}(\mathbf{S})\mathbf{I}]$, and S_{ij} is the strain rate tensor:

$$S_{ij} = \frac{1}{2}\left(\frac{\partial v_i}{\partial x_j} + \frac{\partial v_j}{\partial x_i}\right). \quad (5)$$

In the reference book of Williams [19], there is a more detailed approximation theory of multifluid viscosity. We implement Neumann boundary conditions with reflecting boundary state at the walls for the x-velocity component. We consider compressible flows coupling the concentration equation actively into the flow dynamics. The mixing problems which we study are driven by acceleration-driven forces. The classical Rayleigh-Taylor instability with mixing regime is defined by steady acceleration of a density discontinuities. The Atwood number $A = (\rho_2 - \rho_1)/(\rho_2 + \rho_1)$, with $A > 0$, is an important parameter to measure the effective buoyancy and thus the acceleration of the flow. See the overview in [20]. In this single-mode Rayleigh-Taylor 3D simulation, we update the numerical tool *FronTier* which is based on a front tracking algorithm with a high-quality treatment of a fluid interface with volume fraction formulas. This code is validated [21]. In detail, we developed a local grid-based method, one of the front tracking methods with the volume fraction formulas. A front grid (a codimension 1 grid) specifies a fluid discontinuity location. Through a regular rectangular grid, the front moves freely. In the interface and grid cells, the volume fraction formula is very effective for conserving the mass fractions. At the front, Riemann solutions, which are constructed in a normal direction, provide the physics-based dynamics to move the front at each time step.

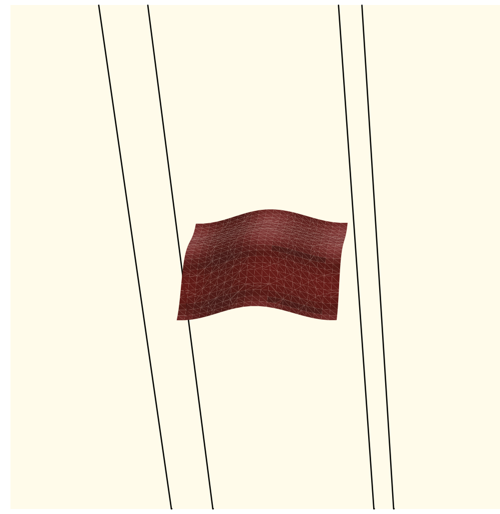

Figure 2: Plot of the interface between the heavy (above) and light (below) fluids at initial time for Rayleigh-Taylor fluid instability. For this study, density ratio is 2 : 1, the Atwood number is 1/3, the peak to peak amplitude of initial disturbance is 0.06, grid size is 20 × 20 × 200, and computational domain is 1 cm × 1 cm × 10 cm.

2. Multiscale Modeling of Single-Mode 3D RT Instability

We simulate 3D single-mode Rayleigh-Taylor with nonzero transport and obtain the surface area with averaged volume fraction formulas. It was already observed [22] without averaged volume fraction formulas; the interface for a related but distinct 2D Richtmyer-Meshkov instability has a length proportional to Δx^{-1}, with respect to its mesh (non)convergence (i.e., rate of divergence) properties.

The mechanism of the interfacial instabilities is the following. The amplitude of mode is 0.1, the phase of mode is 270 degrees, and the boundary type of perturbation in direction is periodic. We show in Figures 2–5 several time steps in the evolving flow. Here, we used transport coefficients for water (Navier-Stokes viscosity: 0.00085105 cm^2/ms, Navier-Stokes mass diffusion: 0.00016366 cm^2/ms, and Navier-Stokes thermal conductivity: 0.00112 cm^2/ms).

In the interface surface area in Figure 6, we observed that the surface area is divergent with time (expressed unphysical units) in three mesh refinements. We convert the surface area to mesh units following the formula

$$\begin{aligned}\frac{(\text{interfacesurface})}{(\text{mixingzonevolume})} &= \frac{\text{physical surface area}/\Delta X * \Delta Y}{(h_{\max} - h_{\min}) * \text{domain}X * \text{domain}Y/\Delta X * \Delta Y * \Delta Z} \\ &= \frac{(\text{physical surface area}) * \Delta Z}{(h_{\max} - h_{\min}) * \text{domain}X * \text{domain}Y}.\end{aligned} \quad (6)$$

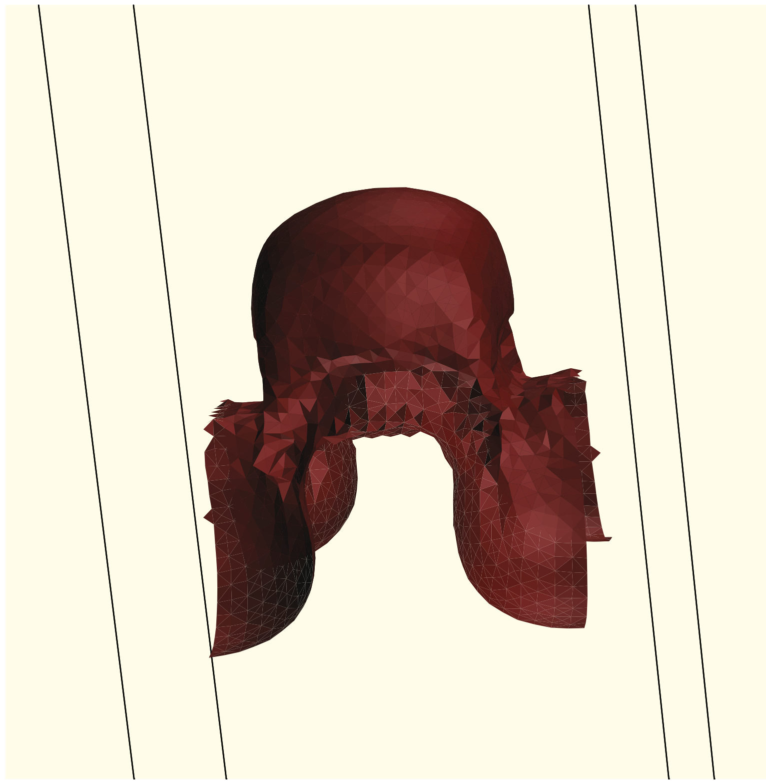

FIGURE 3: Plot of early time for Rayleigh-Taylor fluid instability. Flow and grid parameters as in Figure 2.

FIGURE 4: Plot of middle time for Rayleigh-Taylor fluid instability. Flow and grid parameters as in Figure 2.

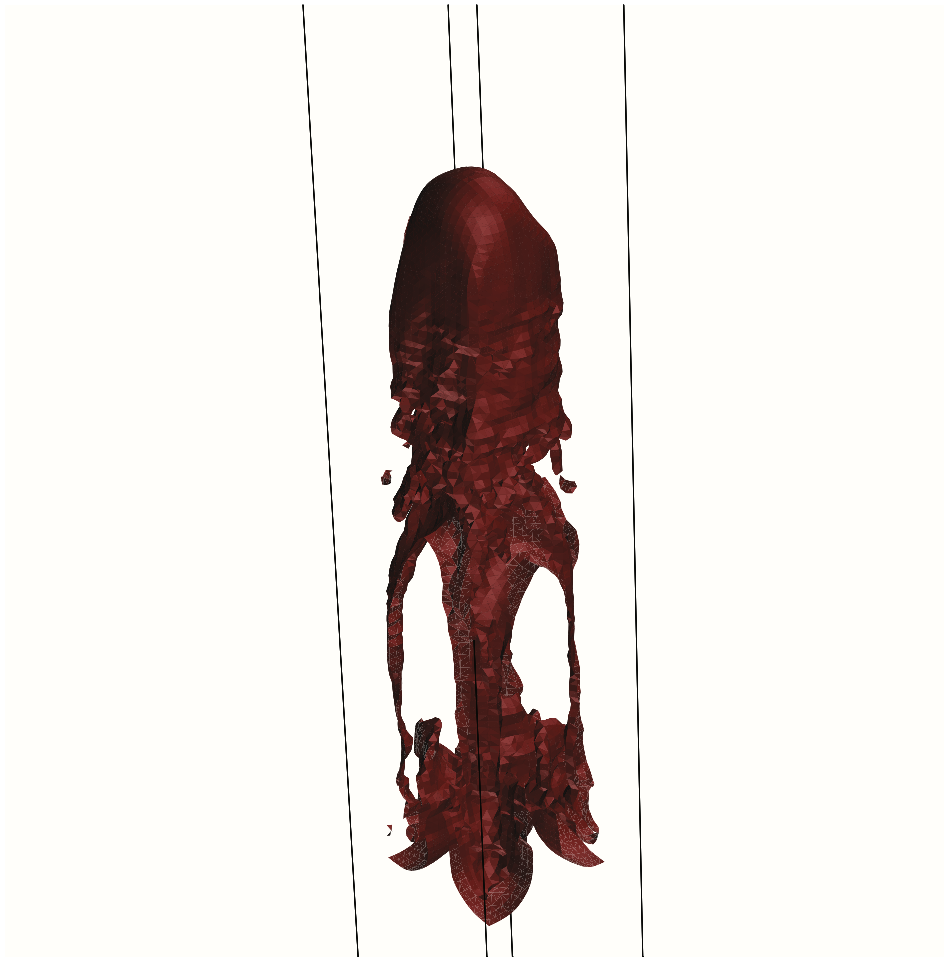

Figure 5: Plot of late time for Rayleigh-Taylor fluid instability. Flow and grid parameters as in Figure 2.

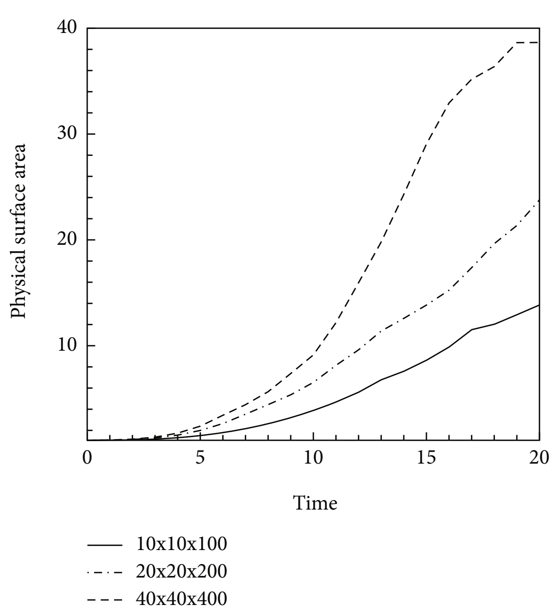

Figure 6: Plot of the interface surface area vs. time using physical units. Results for three mesh levels are displayed for the identical 3D single-mode RT instability.

Here, h_{max} is the maximum height, and h_{min} is the minimum height in the mixing zone. We observe the chaotic interface behavior in Figure 7. By (6), at late time, the mesh fraction of surface area per mixing zone mesh block ranges from 24% to 14%. We interpreted these members as indicating that the flow is a mixture of chaotic patches and nonchaotic patches.

The flow morphology of a single-mode Rayleigh-Taylor disturbance is far less chaotic than a comparison multimode 2D Richtmyer-Meshkov flow, but there is still vortex shedding from the mushroom caps. The flow is more or less chaotic in these vortex shedding regions at late time. So, we study the chaotic flow near the bottom of the mushroom caps and the top of the spike tips in more detail [23].

The mesh level surface fraction is time independent. In the later time, the mesh level surface fraction is about 20% relative to the mixing zone itself. The divergent nature prototypical error analysis of the interface without transport physics is proposed as a formula form [23]:

$$\text{Error} = C_1 \times \Delta x \times (\text{interface area}) = C_1 C_2. \qquad (7)$$

C_i are $\mathcal{O}(1)$ constants independent of Δx. C_1 is related to numerical mass diffusion and might be taken as 3.0 for a typical numerical algorithm [24]. In the single-mode 3D

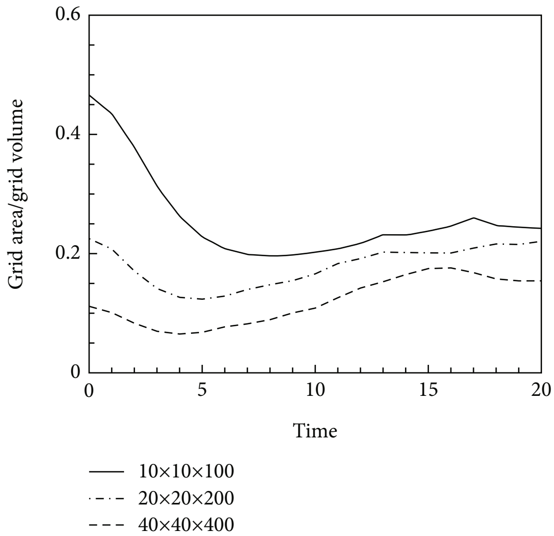

Figure 7: Plot of the interface area divided by the mixing zone volume vs. time. Both the area and the volume are measured in mesh units (the quantity [physical area/physical volume] × Δx is plotted). Results for three mesh levels are displayed for a 3D single-mode RT instability.

Table 1: Table relating Re and λ_K to $\mathrm{Re}_{\mathrm{mesh}}$ at $t = 11.0$ for several mesh levels. Kolmogorov scale $\lambda_{K\mathrm{mesh}} = \lambda_K/\Delta x$. Schmidt number $S c = 5.2$.

Grid size	Re	$\mathrm{Re}_{\mathrm{mesh}}$	$\lambda_{K\mathrm{mesh}}$
$10 \times 10 \times 100$	731.50	32.51	1.22
$20 \times 20 \times 200$	937.04	21.09	1.71
$40 \times 40 \times 400$	1212.36	12.55	2.80

problem and for grid levels considered here, C_2 has a value in the range 0.14 to 0.24.

To study the convergence and mesh refinement, we define $\mathrm{Re} = VL/<\nu>$, ν is the kinematic viscosity, and $<\cdot>$ is an ensemble average. V is the turbulent fluid velocity, $V = \sqrt{<\delta V^2>}$. Here, $\delta V_z = V_z - <V_z>$ is the fluctuating part of the velocity, and L is the mixing zone height $(h_{\max} - h_{\min})$. In the simulation, we used a constant dynamic viscosity. We also use the mesh Reynolds number $\mathrm{Re}_{\mathrm{mesh}} = V\Delta x/<\nu>$ and the Schmidt number $Sc = \nu/\mu$ as a new dimensionless parameter, where μ is the coefficient of molecular mass diffusion. The Kolmogorov length scale $\lambda_K = (\nu^3/\varepsilon)^{1/4}$ or the viscous inner scale, approximately $50\lambda_K$, is a measure of the lengths at which viscosity plays a role, and this is related to the level of mesh refinement needed for a numerical simulation. For comparison, Δx for the finest grid is comparable to λ_K and well below the inner viscous scale, indicating that the calculation is in close to fully resolved simulation. We need to do more mesh refinement to get fully resolved simulation. Here, ε is the dissipation rate:

$$\varepsilon = \frac{\nu}{2} \left\| S_{ij} \right\|_2^2, \tag{8}$$

where S_{ij} is (5). See Table 1 relating Re and λ_K to $\mathrm{Re}_{\mathrm{mesh}}$.

3. Conclusions

In this paper, we investigate the simulation of a single-mode Rayleigh-Taylor instability with the volume fraction formulas in 3D. By the implementation of surface area function, we can precisely observe the chaotic behavior of the interface flow. The flow morphology is far less chaotic than a comparison 2D multimode Richtmyer-Meshkov flow. There is still vortex shedding from the mushroom caps, at which locations of the flow are more or less chaotic. So, we can study the chaotic flow of the bottom of the mushroom caps and the top of the spike tips in more detail. Here, we studied the Kolmogorov length scale which is relative to the level of mesh refinement for numerical simulation. Finally, in the future work, we will apply Prandtl and Batchelor scales which are need to resolve more fully for numerical simulation.

Data Availability

This data is available from this paper. If you need to have further information, then, send an email to the author.

Disclosure

Some research progress was presented in the KMS conference (https://www.kms.or.kr/).

Conflicts of Interest

The author declares that we have no conflict of interest. The author is the dual faculty of Phoenix College and Sonoran Schools.

Acknowledgments

Prof. Sheen is my coresearcher not in this work but in another work (An Exact Method to Find a Circle Passing through Two Points and Minimizing the Maximal Weighted Distance to a Set of Points, Computers and Operations Research, vol. 40, issue 5, Pages 1300-1305, May, 2013).

References

[1] J. Glimm, J. Grove, X. Li, K.-M. Shyue, Q. Zhang, and Y. Zeng, "Three-dimensional front tracking," *SIAM Journal on Scientific Computing*, vol. 19, no. 3, pp. 703–727, 1998.

[2] V. Rutka and Z. Li, "An explicit jump immersed interface method for two-phase Navier-Stokes equations with interfaces," *Computer Methods in Applied Mechanics and Engineering*, vol. 197, no. 25-28, pp. 2317–2328, 2008.

[3] Y. Kim and C. Peskin, "3-D parachute simulation by the immersed boundary method," *Computers and Fluids*, vol. 38, no. 6, pp. 1080–1090, 2009.

[4] C. Peskin, "Numerical analysis of blood flow in the heart," *Journal of Computational Physics*, vol. 25, no. 3, pp. 220–252, 1977.

[5] P. Colella and P. R. Woodward, "The Piecewise Parabolic Method (PPM) for gas-dynamical simulations," *Computers in Physics*, vol. 54, no. 1, pp. 174–201, 1984.

[6] R. Fazio and R. J. LeVeque, "Moving-mesh methods for one-dimensional hyperbolic problems using CLAWPACK," *Computers & Mathematics with Applications*, vol. 45, no. 1-3, pp. 273–298, 2003.

[7] Y. Chang, T. Hou, B. Merriman, and S. Osher, "A level set formulation of Eulerian interface capturing methods for incompressible fluid flows," *Journal of Computational Physics*, vol. 124, no. 2, pp. 449–464, 1996.

[8] J. Grooss and J. Hesthaven, "A level set discontinuous Galerkin method for free surface flows," *Computer Methods in Applied Mechanics and Engineering*, vol. 195, no. 25-28, pp. 3406–3429, 2006.

[9] J. Kim, "A continuous surface tension force formulation for diffuse-interface models," *Journal of Computational Physics*, vol. 204, no. 2, pp. 784–804, 2005.

[10] M. Francois and W. Shyy, "Computations of drop dynamics with the immersed boundary method, part 1: numerical algorithm and buoyancy-induced effect," *Numerical Heat Transfer: Part B: Fundamentals*, vol. 44, no. 2, pp. 101–118, 2003.

[11] M. Francois, E. Uzgoren, J. Jackson, and W. Shyy, "Multigrid computations with the immersed boundary technique for multiphase flows," *International Journal of Numerical Methods for Heat & Fluid Flow*, vol. 14, no. 1, pp. 98–115, 2004.

[12] Y. Kim and C. Peskin, "Numerical study of incompressible fluid dynamics with nonuniform density by the immersed boundary method," *Physics of Fluids*, vol. 20, no. 6, article 062101, 2008.

[13] A. Banerjee, "Rayleigh-Taylor instability: a status review of experimental designs and measurement diagnostics," *Journal of Fluids Engineering*, vol. 142, pp. 12080–12117, 2020.

[14] N. T. Clemens and M. G. Mungal, "Large-scale structure and entrainment in the supersonic mixing layer," *Journal of Fluid Mechanics*, vol. 284, pp. 171–216, 1995.

[15] J. D. Lindl, "Development of the indirect-drive approach to inertial confinement fusion and the target physics basis for ignition and gain," *Physics of Plasmas*, vol. 2, no. 11, pp. 3933–4024, 1995.

[16] D. Livescu, "Numerical simulations of two-fluid turbulent mixing at large density ratios and applications to the Rayleigh–Taylor instability," *Philosophical Transactions of the Royal Society*, vol. 371, 2013.

[17] D. Kim, *Conservative Data Collections and Comparison Study for Front-Tracking [Ph.D Dissertation]*, Applied Mathematics and Statistics, Stony Brook University, 2009.

[18] T. Barberon and P. Helluy, "Finite volume simulation of cavitating flows," *Computers and Fluids*, vol. 34, no. 7, pp. 832–858, 2005.

[19] F. Williams, *Combustion Theory*, Addison-Wesley Co., 1965, Reading.

[20] D. H. Sharp, "An overview of Rayleigh-Taylor instability," *Physica D: Nonlinear Phenomena*, vol. 12, no. 1-3, pp. 3–18, 1984.

[21] https://github.com/frontier-sunysb/FronTier.

[22] H. Lee, H. Jin, Y. Yu, and J. Glimm, "On validation of turbulent mixing simulations for Rayleigh-Taylor instability," *Physics of Fluids*, vol. 20, no. 1, pp. 012102–012108, 2008.

[23] H. Lim, Y. Yu, H. Jin et al., "Multiscale models for fluid mixing," *Computer methods in applied mechanics and engineering*, vol. 197, no. 43-44, pp. 3435–3444, 2008.

[24] S. Dutta, J. Glimm, J. W. Grove, D. H. Sharp, and Y. Zhang, "Error comparison in tracked anduntracked spherical simulations," *Computers and Mathematics with Applications*, vol. 48, no. 10-11, pp. 1733–1747, 2004.